Reorganized atmospheric circulation during the Little Ice Age leads to rapid Southern California deoxygenation

Yi Wang[1], Ingrid L. Hendy[1]

[1]Department of Earth and Environmental Sciences, University of Michigan, Ann Arbor, MI, USA

Corresponding author: Yi Wang (ellawang@umich.edu).

Abstract

The magnitude of natural oceanic dissolved oxygen (DO) variability remains poorly understood due to the short duration of the observational record. Here we present a high-resolution (4–9 years) reconstruction of the Southern California oxygen minimum zone (OMZ) through the Common Era using redox-sensitive metals. Rapid OMZ intensification on multidecadal timescales reveals greater DO variability than observed in instrumental records. An anomalous interval of intensified OMZ between 1600–1750 CE contradicts the expectation of better-ventilated mid-depth North Pacific during cool climates. Although the influence of low-DO Equatorial Pacific Intermediate Water on the Southern California Margin was likely weaker during this interval, we attribute the observed rapid deoxygenation to reduced North Pacific Intermediate Water (NPIW) ventilation. NPIW ventilation thus appears very sensitive to atmospheric circulation reorganization (e.g., a weakened Siberian High and Aleutian Low). In addition to temperature-induced gas solubility, atmospheric forcing under future anthropogenic influences could amplify OMZ variability.

Plain Language Summary

Oxygen content of the ocean is declining as seawater warms due to anthropogenic climate change impacting gas solubility. However, how much dissolved oxygen in seawater can decrease naturally is unknown, as we have only been measuring oxygen in ocean waters for ~60 years. We reconstructed oxygen concentrations of bottom waters in Santa Barbara Basin (SBB), CA for the past 2000 years using marine sediments on sub-decadal time scales. We found that seawater oxygen varied more in the past than has been

This is the author manuscript accepted for publication and has undergone full peer review but has not been through the copyediting, typesetting, pagination and proofreading process, which may lead to differences between this version and the Version of Record. Please cite this article as doi: 10.1029/2021GL094469.

recently observed, and that seawater oxygen was surprisingly low during 1600–1750 CE — one of the coldest intervals during the last 1000 years. At this time the atmospheric circulation over the Sea of Okhotsk suppressed sea ice formation, reducing the surface ocean mixing that supplies oxygen to the subsurface waters. This low-oxygen subsurface water moved around the northeastern Pacific Ocean and entered SBB. The sensitivity of this process to atmospheric circulation could generate additional seawater oxygen variability. Future projections of ocean oxygen should take these results into account.

Key points

1. Rapid Southern California oxygen minimum zone (OMZ) intensification reveals greater variability than that in post-Industrial reconstruction.
2. Intensified OMZ during the Little Ice Age (LIA) contradicts the expectation of better-ventilated mid-depth North Pacific in cool climate.
3. OMZ intensification in LIA was due to reduced North Pacific Intermediate Water ventilation under a weakened Aleutian Low and Siberian High.

Introduction

Marine dissolved oxygen (DO) is controlled by both O_2 supply and consumption. Observed subsurface ocean DO deficiencies since the mid-20th century have been attributed to a warming ocean, which reduces O_2 supply by decreasing O_2 solubility in surface waters and increasing water column stratification (Bopp et al., 2013; Breitburg et al., 2018; Stramma et al., 2010). The warming trend may also enhance subsurface O_2 consumption by increasing organic carbon respiration rates in the water column (Carstensen et al., 2014). An additional mechanism to supply O_2 to the ocean interior is through ventilation. During this process, well-oxygenated surface waters that exchange air with the atmosphere sink to form subsurface water masses as density increases due to cooling and/or increased salinity, thereby supplying DO to the ocean interior. Once subsurface water masses are isolated from the atmosphere and free to circulate in the ocean, DO decreases with persistent O_2 consumption via respiration.

Intermediate water ventilation changes under climate change can control subsurface DO, which in turn can cause Northeast Pacific oxygen minimum zones (OMZs) to expand and contract (Behl and Kennett, 1996; Cannariato and Kennett, 1999;

Hendy and Pedersen, 2005; Ivanochko and Pedersen, 2004). Greater intermediate water ventilation during the cool Last Glacial weakened OMZs in the NE Pacific Ocean; in contrast suppressed intermediate water formation during warmer climate states (e.g., interstadials and interglacials) strengthened OMZs (Hendy and Pedersen, 2005; Ivanochko and Pedersen, 2004; Keigwin, 1998). Remote control of Southern California OMZ by North Pacific intermediate water (NPIW) ventilation has been associated with atmospheric forcing (Wang et al., 2020). For instance, weakened OMZs during the mid- to late-Holocene (Moffitt et al., 2015; Ohkushi et al., 2013) were observed when atmospheric circulation favored greater NPIW formation (Wang et al., 2020). Ventilation of NPIW, however, is poorly constrained on the annual to decadal timescales under which marine resource managers operate.

Redox-sensitive metal precipitation in sediments can be used to reconstruct DO prior to observational data, if DO concentrations at the sediment-water interface control porewater redox conditions (Calvert and Pedersen, 2007). Here we use authigenic enrichment factors of Mo_{EF}, $Re_{EF,}$ and Ba_{EF} with respect to the lithogenic background to reconstruct past oxygenation. With an extremely low crustal concentration, rhenium is conservative in oxygenated waters, but precipitates when reduced under low-oxygen conditions (Crusius et al., 1996; Tribovillard et al., 2006). Molybdenum primarily exists as conservative molybdates, despite scavenging by Mn (oxyhydr)oxides in oxygenated waters (Scott et al., 2008) and complexation with dissolved organic carbon (Tessin et al., 2018; Wagner et al., 2017). However, when free sulfide (HS^-) is present, molybdate is converted to thiomolybdate that is readily scavenged into sediments (Erickson and Helz, 2000). Mo can thus be used as an indicator of strongly reducing conditions (i.e., sulfidic environments with HS^- presence) provided that coeval Re enrichments are observed (Calvert and Pedersen, 2007; Tribovillard et al., 2006; Zheng et al., 2000). Finally, barite forms on decaying organic particles in oxygenated water columns. If deposited in sulfidic porewaters, barite readily dissolves and releases free Ba^{2+} into porewaters, resulting in sedimentary Ba depletion (Griffith and Paytan, 2012; Hendy, 2010; McManus et al., 1998; Torres et al., 1996; Von Breymann et al., 1992). However, diagenetic barite re-precipitation is likely to occur when free Ba^{2+} reacts with SO_4^{2-} (Supplementary Information Text S3). Through this diagenetic process, positive Ba_{excess} in reducing

sediments support relatively oxygenated porewaters that allowed barite preservation, and thus it can be used as an indicator of better oxygenated environments when Ba_{excess} coincides with low Mo_{EF} and Re_{EF}.

Located on the Southern California margin, the Santa Barbara Basin (SBB) connects to the broader Southern California OMZ over a 475-m western sill. Below the sill depth in the basin, DO is depleted by respiration of local upwelling-driven export productivity (Checkley and Barth, 2009; Moffitt et al., 2014). SBB bottom waters have low to non-detectable oxygen (anoxic) concentrations (typically < 20 μmol/kg) that suppress mega/macrofaunal activity to enable annually laminated sediment preservation. SBB is actively ventilated by water entering the basin over the western sill during the 'flushing events', as better-oxygenated and dense intermediate waters from the OMZ displace bottom waters in the basin (Bograd, 2002; Goericke et al., 2015). Here we present a 2000-year high-resolution (4–9 years) redox-sensitive trace metal record from the SBB to constrain natural DO variability on sub-decadal to millennial timescales in Southern California. This Common Era (CE) record should reveal the magnitude of natural Southern California OMZ shifts relative to anthropogenic influences. We further explore Southern California OMZ responses to remote intermediate water ventilation and associated atmospheric forcing in the CE (Fig. 1), by comparing proxy records and simulated climatology from the Last Millennium Reanalysis (LMR) that incorporates proxy information into climate model simulated data (Supplementary Information Text S2) (Hakim et al., 2016; Tardif et al., 2019).

2 Materials and Methods

2.1 Geochemical measurements and enrichment factors

The Kasten core SPR0901-03KC (34°16.990'N, 120°2.408'W; 586 m depth) uses a well-constrained age model based on a companion core SPR0901-06KC (Du et al., 2018; Hendy et al., 2013). An age-depth model of 06KC was generated using Bacon 2.2 from 49 mixed planktonic foraminiferal ^{14}C dates and varve counting for the last 300 years (Hendy et al., 2015; Schimmelmann et al., 1992). Foraminiferal ^{14}C dates were calibrated using the Marine13 curve (Reimer et al., 2013) and varying reservoir ages

(Hendy et al., 2013). The 06KC age-depth model was then mapped onto 03KC using 31 tie points (e.g., turbidites, flood layers, and visually distinct varves) (Wang et al., 2019).

03KC was sampled continuously at 2-mm intervals (~2 years resolution), freeze-dried and ground to generate bulk samples. Core samples corresponding to 950–1150 and 1350–1850 CE were analyzed for elemental concentrations at a 4-mm resolution, while the remainder of the core was analyzed at 8 mm resolution. Approximately 10–15 mg of the bulk sample was weighed (~300 samples in total) and digested using an acid cocktail of 0.8 mL HNO_3, 0.1 mL HCl, and 0.2 mL HF in the MARS 6 (CEM Corporation, North Carolina) microwave digestion system for 20 min at 180 °C. Solutions were evaporated and re-dissolved in 1.5 M HCl for elemental analysis on a Thermo iCAP Q inductively coupled plasma mass spectrometer (ICP-MS) at the Michigan Elemental Analysis Lab (MEAL), University of Michigan. MESS-3, PACS-2, and HISS-1 sediment reference materials were used to monitor element recoveries (Table S1). The relative standard deviation (RSD) for the three measurements of each sample was < 10% on the Thermo iCAP Q.

Enrichment factors ($Metal_{EF}$) with respect to the lithogenic background were calculated by normalizing redox-sensitive trace metal concentrations to Al (Eq. 6-1):

$$Metal_{EF} = \frac{(Metal / Al)_{sample}}{(Metal / Al)_{background}} \qquad \text{(Eq. 6-1)}$$

Lithogenic background was derived from the elemental concentrations of bedload samples from the Santa Clara and Ventura Rivers, and the Santa Rosa Islands (Napier et al., 2019), which were then weighted based on the respective sediment transport flux into the SBB (Warrick and Farnsworth, 2009) as discussed in detail in Wang et al. (2017). Barium was corrected for the detrital input ($Ba_{excess} = Ba_{sample} - (Ba/Al)_{background} \times Al_{sample}$) with the background from Wang et al. (2017).

The Last Millennium Reanalysis (LMR) was used to identify atmospheric circulation shifts (Supplementary Information Text S2) (Hakim et al., 2016; Tardif et al., 2019). All climate variables were converted to anomalies with respect to the 0–1850 CE mean for comparison. All ages are in CE henceforth.

3 Rapid Southern California OMZ oscillations during the Common Era compared to the Post-Industrial

The expected correspondence between the climate and DO is broadly observed in the new record (Fig. 2). Redox metal enrichments in SBB sediments including the highest Mo_{EF} (occurring between 940–1050 and 1100–1160, Fig. 2) were coincident with the Medieval Climate Anomaly (MCA), an interval in which Northern Hemisphere climate is generally considered to be warm (PAGES 2k Consortium, 2013). High upwelling diatom and silicoflagellates (Barron et al., 2015), and anchovy (Skrivanek and Hendy, 2015) abundances are observed during these intervals, indicating stronger coastal upwelling. Enhanced export productivity associated with upwelling should consume DO in the ambient waters via organic matter decay, likely contributing to the extreme reducing conditions between 940–1050 and 1100–1160. In contrast, the most oxygenated interval (1250–1500) of the new record occurred during the transition to the early Little Ice Age (LIA), when cool subpolar planktic foraminiferal species appeared in the basin (Fisler and Hendy, 2008). Low $Metal_{EF}$ coinciding with positive Ba_{excess} suggested that porewaters during this interval contained sufficient oxygen to preserve barite (Fig. 2a). Southern California OMZ intensification during relatively warm intervals (e.g., 940–1050 and 1100–1160) and relaxation during the cool intervals (1250–1500) (Fig. 2) is consistent with the climate-related ventilation control on the Southern California OMZ observed over the past 60 ka (Behl and Kennett, 1996; Cannariato and Kennett, 1999; Hendy and Pedersen, 2005; Ivanochko and Pedersen, 2004), when a better ventilated mid-depth Pacific occurred during cool climates.

The abrupt OMZ intensification between 940–1120 during the MCA (Mo_{EF} of 11.24 and 7.51, Fig. 2c) represents the highest Mo_{EF} recorded in SBB throughout the Holocene (Wang et al., 2020) and indicates more reducing conditions than the post-Industrial Southern California OMZ intensification (Wang et al., 2017) (Fig. 2d).This OMZ intensification occurred rapidly on a multi-decadal timescale. Although Mo_{EF} responses to DO may not be linear, a qualitative estimate of the Southern California OMZ intensification and relaxation rates highlights the natural speed of change in OMZ variability. OMZ intensification/relaxation intervals were selected based on the turning points of the 5-point Mo_{EF} moving average (Supplementary Information Text S4). Only intervals with more than 5 data points and statistically significant correlation coefficients

(on 5% significance level) are reported here (Fig. 2). Both OMZ intensification and relaxation in the CE can be as short as several decades. Intensification rates (Mo_{EF} slope of 0.09 ± 0.06 [SD]/year) were usually faster than relaxation rates (Mo_{EF} slope of -0.05 ± 0.01 [SD]/year), and all were faster than during the post-Industrial OMZ expansion (Fig. 2, Wang et al., 2017). The OMZ intensification rate (0.20/year) between 946–986 was the most significant of the CE, higher than the recent expansion of the 20th century (0.04/year for 1927–1969, Fig. 2d). Such high-frequency OMZ oscillations demonstrates the rapid (de)oxygenation under natural climate change that has not yet been revealed in the post-Industrial sedimentary record.

4 Rapid Southern California deoxygenation in the late LIA and remote water mass influences

Despite the general correspondence between better ventilated OMZ and cooler climate, OMZ relaxation abruptly terminated at ~1500 as positive Ba_{excess} ceased, followed by a transition into the low-oxygen interval between 1600 and 1750, when Re_{EF} and Mo_{EF} again increased above average (Fig. 2b-c). During this low-oxygen interval, global mean surface temperature reconstructions indicate a ~0.4 °C cool anomaly with respect to 1961–1990 (Neukom et al., 2019a), making it the coldest interval of the CE in the eastern and central Pacific (Neukom et al., 2019b). This late LIA low-oxygen interval thus seems to contradict the observed relationship between cool climate and better-ventilated Southern California OMZ (Behl and Kennett, 1996; Cannariato and Kennett, 1999; Hendy and Pedersen, 2005). The absence of strong evidence for local oxygen consumption via increased export productivity (Barron et al., 2015; Wang et al., 2019) (Fig. 2e) indicates that remote water mass ventilation may have played a significant role.

4.1 Weakened Equatorial Pacific Intermediate Water advection to the Southern California margin in the late LIA

Remote water mass influences on the Southern California OMZ are associated with either Equatorial Pacific Intermediate Water (EqPIW) and/or North Pacific Intermediate Water (NPIW) (Fig. 1). Both ventilation/O_2 consumption shifts during the intermediate water formation and/or advection of intermediate waters to the basin could affect DO (Crusius et al., 2004). EqPIW oxygenation and advection to the California Margin can be evaluated by the presence of denitrified water from the Eastern Tropical

North Pacific (ETNP) OMZ (Deutsch et al., 2014; Evans et al., 2020; Tems et al., 2015; Tems et al., 2016; Wang et al., 2019). Sedimentary $\delta^{15}N$ ($\delta^{15}N_{sed}$) is a record of upper water column nitrate $\delta^{15}N$, which is transported to the sediments via the sinking organic matter. High $\delta^{15}N_{sed}$ values from the Pescadero Slope, Gulf of California (PESC-GC3, 24°16.759'N, 108°11.700'W, 620 m water depth, Fig. 1) have been attributed to intensified water-column denitrification in the ETNP OMZ (Fig. 3a) (Tems et al., 2016). The elevated ETNP $\delta^{15}N_{sed}$ signal can subsequently be transported to the Southern California margin via the California Undercurrent (CUC) (Altabet et al., 1999; Kienast et al., 2002; Liu and Kaplan, 1989; Tems et al., 2015; Wang et al., 2019). $\delta^{15}N_{sed}$ has thus been used as a tracer of the southern-sourced denitrified water transport into the Southern California (Davis et al., 2019; Tems et al., 2015; Wang et al., 2019). To evaluate the ETNP denitrified water influences, a rolling correlation (Fig. S6) of the Pescadero slope (Tems et al., 2016) and the SBB $\delta^{15}N_{sed}$ (Wang et al., 2019) (Fig. 3) is used to identify in-phase/out-of-phase variability (Supplementary Information Text S5). Although $\delta^{15}N_{sed}$ is affected by local water-column denitrification regulated by DO, SBB $\delta^{15}N_{sed}$ is primarily a reflection of ETNP water transport via the CUC but not a DO proxy, which is supported by the SBB sediment trap series (Davis et al., 2019). Inconsistencies (e.g., notably during LIA, Fig. 3b and c) with redox-sensitive trace metals that reflect the bottom water DO via porewaters (Wang et al., 2017) further relate SBB $\delta^{15}N_{sed}$ to changes in this ETNP denitrified water transport.

When the two $\delta^{15}N_{sed}$ records are in phase, the Southern California OMZ is likely influenced by denitrified water advected from the ETNP; while when the out-of-phase relationship is observed, a weakened ETNP water influence is suggested (Wang et al., 2019). Coeval high $\delta^{15}N_{sed}$ values in the SBB and on the Pescadero Slope during 950–1150 are consistent with high SBB redox-sensitive metal enrichments (Figs. 3a-c), supporting low-O_2 EqPIW influences on the Southern California OMZ. However, denitrified EqPIW influence on the Southern California margin appears to weaken as the climate cools into the late LIA, as indicated by a transition to more frequent out-of-phase behavior after ~1550 (Figs. 3a-b and S6). During the low-oxygen interval between 1600 and 1750, the relatively high Pescadero Slope $\delta^{15}N$ values are out of phase with the low SBB $\delta^{15}N$ values, indicating weakened ETNP denitrified water transport and ventilation

of the Southern California OMZ likely dominated by NPIW. This interval also stands out with a decoupling of low $\delta^{15}N_{sed}$ from the high redox-sensitive metal enrichments in SBB (Fig. 3), further supporting likely changes in the upper water column nitrate source. It thus appears that low-O_2 EqPIW is not the primary driver for the sustained low-oxygen conditions during the late LIA. Reduced EqPIW transport could have increased the relative contribution of NPIW influences on the Southern California Margin.

4.2 Reorganized atmospheric circulation drives poorly ventilated North Pacific Intermediate Water during the late LIA

NPIW currently ventilates in the Sea of Okhotsk when heat- (e.g., surface cooling) or salinity-driven (e.g., sea ice brine rejection) buoyancy loss of surface water forms dense Okhotsk Sea Intermediate Water (Supplementary Information Text S1). This well-oxygenated intermediate water mass is exported by subarctic Oyashio waters, which merge with the subtropical Kuroshio Extension east of Japan to produce NPIW that propagates across the mid-depth North Pacific (Talley, 1993; Yasuda, 1997). Despite the cooler climate conditions in the late LIA (Neukom et al., 2019a), simulations from the Last Millennium Reanalysis (LMR) show only a minor Sea of Okhotsk sea surface temperature (SST) anomaly (<0.1 °C with respect to the 0–1850 mean, Fig. 4a) between 1550 and 1750 (Southern California OMZ intensification, Fig. 3a-d), indicating that heat-driven buoyancy loss was unlikely to significantly affect NPIW ventilation. However, more buyont surface waters in the Sea of Okhotsk driven by reduced sea ice formation may have weakened NPIW ventilation during this interval. Low abundances of the sea-ice related radiolarian *Cycladophora davisiana* (Itaki, 2004; Okazaki et al., 2006) suggests a sea ice decline between ~1600–1750 (Fig. 3d). Reduced sea ice is also supported by the relatively low abundance of sea-ice related diatom (e.g., *Bacterosira fragiles* and *Fragilariopsis cylindrus*) species during ~1450–1800 (Koizumi et al., 2003; Shimada et al., 2004).

In addition to SSTs, atmospheric circulation (relative position and intensity of the Aleutian Low [AL] and Siberian High [SH]) over the Sea of Okhotsk also regulates sea ice formation (Parkinson, 1990; Tachibana et al., 1996). A strengthened AL usually shifts southeastward, centering south of the Alaska Peninsula (Rodionov et al., 2007). Along with an intensified SH, northerly or northwesterly winds produce polynyas by moving

sea ice away from the northern shelf of the Sea of Okhotsk. Polynyas facilitate dense water formation on the shelf by exposing open water to subzero air temperatures and surface winds, leading to greater sea ice formation and brine rejection, ultimately increasing salinity-driven buoyancy loss (Martin et al., 1998). Conversely, a weak AL often splits into two centers, residing in the Northwest Pacific and the Gulf of Alaska (Fig. 1) (Rodionov et al., 2007). Declining Okhotsk sea ice is thus associated with reduced wind stress caused by weakened AL/SH and easterly winds that suppress polynya formation under westward AL (Parkinson, 1990; Tachibana et al., 1996).

Multiple proxy records have shown westward and/or weakened AL during the late LIA. Relatively enriched sedimentary calcite oxygen isotopic composition ($\delta^{18}O_{Ca}$) of Jellybean Lake, Yukon Territory indicates a westward/weakened AL between 1550–1800 (Anderson et al., 2005) (Fig. 3e). This observation is consistent with enriched diatom $\delta^{18}O$ in the Heart Lake, Aleutian Islands between 1550–1700 (Bailey et al., 2018), and reduced sea salt aerosol in ice core records from Mt. Logan, Yukon Territory and Denali between ~1540–1700 (Osterberg et al., 2014; Osterberg et al., 2017). Proxy reconstructions of AL are also supported by the Last Millennium Reanalysis (LMR) product. Slightly positive average sea level pressure (SLP) anomalies during 1550–1750 in the central North Pacific and negative anomalies over the Gulf of Alaska and Sea of Okhotsk suggest a weaker/westward centered AL (Fig. 4b), which may have led to prevailing easterlies over the Sea of Okhotsk and suppressed polynya formation. Negative SLP and 500 hPa geopotential height anomalies over the Siberia further indicates that a weakened SH contributed to reduced wind stress over the Sea of Okhotsk (Fig. 4b and S2). Thus, despite the cooler climate during 1550–1750, the Sea of Okhotsk sea ice response to atmospheric forcing (e.g., weakened AL and SH) reduced NPIW ventilation, leading to the propagation of the low-DO signal throughout the mid-depth North Pacific and subsequently Southern California OMZ intensification.

A relatively weak AL and reduced Sea of Okhotsk ice formation prior to 800 CE (Fig. S7), may have led to less ventilated NPIW and Southern California OMZ intensification. However, the Pescadero Slope $\delta^{15}N_{sed}$ is of insufficient length to recover the first millennium, preventing evaluation of the relative importance of EqPIW versus NPIW. Additional high-resolution CE records are required to assess whether atmospheric

circulation forced NPIW ventilation changes could have contributed to rapid OMZ intensification during other intervals of the last two millennia.

5 Conclusions

Observed ocean deoxygenation since the 1950s has initiated discussion of the vulnerability of oxygen minimum zones (OMZs). We present a new Common Era (CE) redox-sensitive metal record from the Santa Barbara Basin (SBB) that reconstructs Southern California OMZ at a 4–9 year resolution. This record indicates that rapid OMZ intensification and relaxation occurred within decades, and post-Industrial OMZ intensification (Wang et al., 2017) is not unprecedented. The current deoxygenation trend could thus be significantly exacerbated if overlaid by synergistic natural OMZ variability.

The overall correspondence between OMZ shifts and climatic events is consistent with a weakened OMZ during cool intervals due to better-ventilated intermediate waters in the North Pacific (Fig. 5). However, 1600–1750 CE in the late Little Ice Age (LIA) stands out as a low-DO interval when the climate was cool, contradicting the conventional prediction of better ventilated intermediate water during cool climates. Poor correlation with local export productivity indicates that OMZ intensification was not driven by O_2 consumption in the basin. Simultaneously, the observed out-of-phase relationship of sedimentary nitrogen isotope records from the SBB and the Pescadero Slope (Tems et al., 2016) reveals a potential weakening of low-DO Equatorial Pacific Intermediate Water (EqPIW) influence on the Southern California Margin (Fig. 5). We thus suggest that the low bottom water DO during 1600–1750 was associated with reduced North Pacific Intermediate Water (NPIW) ventilation caused by suppressed Sea of Okhotsk ice formation (Itaki, 2004). Proxies and the Last Millennium Reanalysis (LMR) indicate that a weaker/westward Aleutian Low and a weakened Siberian High produced prevailing easterly winds over the Sea of Okhotsk, thereby reducing sea ice production and NPIW ventilation. Intermediate water ventilation thus does not have a simple response to air temperature as occurred on orbital and millennial timescales. Given the relatively small temperature changes during the Holocene, North Pacific OMZ variability is instead, very sensitive to large-scale atmospheric circulation shifts.

Figure Captions

Figure 1. Core locations and circulation patterns. (a) Relative position of a westward and/or weakened Aleutian Low (AL) (blue shading) and Siberian High (SH) (orange shading). Dark blue and orange arrows in the AL and SH shading represent wind directions in each pressure system. Red star: Santa Barbara Basin (SBB) marine core (SPR0901-03KC; 34°16.990'N, 120°2.408'W; 586 m water depth); yellow stars: Pescadero Slope marine core (PESC-GC3; 24°16.759'N, 108°11.700'W; 620 m water depth) (Tems et al., 2016), and Sea of Okhotsk marine core (GH01-1011; 44°35.50'N, 144°26.10'E; 1348 m water depth) (Itaki, 2004). Yellow circles: Jellybean lake (Anderson et al., 2005), and Heart Lake cores (Bailey et al., 2018). Red circle: Mount Logan ice core (Osterberg et al., 2014). Intermediate water masses (light gray shading) and the North Pacific Intermediate Water (NPIW) formation regions (dark gray shading and dashed line) (Bostock et al., 2010; Bostock et al., 2013; Talley, 2008). Ocean currents are shown in white arrows. KaC: Kamchatka Current; OyC.: Oyashio Current; KuC.: Kuroshio Current; NEC: North Equatorial Current; CC: California Current; CUC: California Undercurrent; GoA: Gulf of Alaska; AC: Alaska Current; AS: Alaska Stream. NPIW: North Pacific Intermediate Water; NEqPIW: North Equatorial Pacific Intermediate Water. Base map was generated in Ocean Data View.

Figure 2. Common Era oxygenation variability from metal enrichments compared to local export productivity in Santa Barbara Basin. (a) Ba_{excess} (blue lines) with the horizontal dashed line showing zero excess; (b-c) Re (green lines) and Mo (purple lines) enrichment factors from SPR0901-03KC with the horizontal dashed line showing mean values. (d) Calculated OMZ intensification/relaxation rates based on the least-square linear regression of Mo_{EF}. The identified intensification (red bars)/relaxation intervals (blue bars) are labeled with the years of their duration. Solid bars correspond to 03KC while the dashed bar to SPR0901-04BC (Wang et al., 2017); (e) Total organic carbon for the core SPR0901-03KC (Wang et al., 2019). Dashed curves in the panel a-c and e show $Ba_{exces,}$ $Metal_{EF,}$ and TOC (wt. %) from SPR0901-04BC (Wang et al., 2017). Shaded bars represent 'more oxygen' (blue, defined by below average Mo_{EF} values) and 'low oxygen' intervals (orange, defined by above average Mo_{EF} values).

Figure 3. Regional comparison of climate and oxygenation proxies in the North Pacific Ocean. (a) Bulk sedimentary $\delta^{15}N$ (red line) from the Pescadero slope (PESC-GC3; Tems et al. (2016)). (b) Bulk sedimentary $\delta^{15}N$ (pink line) from the SBB (SPR0901-03KC; Wang et al. (2019). (c) Mo (purple line) enrichment factors for core SPR0901-03KC (solid) and SPR0901-04BC (dashed line) (Wang et al., 2017). (d) Relative abundance of *Cycladophora Davisiana* (brown line) in the Sea of Okhotsk (Itaki, 2004). The scale is inverted so high values (down) represent better ventilation. Orange triangles represent mollusca-based ^{14}C age control points; (e) Lake sediment carbonate $\delta^{18}O$ (orange line) in the Jellybean Lake (Anderson et al., 2005); Shaded bars represent 'more oxygen' (blue, defined by below average Mo_{EF} values) and 'low oxygen' (orange, defined by above average Mo_{EF} values). In-phase (black bar at the top) and out-of-phase (gray bar) relationships are determined using 25-point rolling correlation (Supplementary Information Text S5 and Fig. S6).

Figure 4. Last Millennium Reanalysis (Tardif et al., 2019) product analysis. (a) Sea surface temperature (SST) and (b) sea level pressure (SLP) anomaly for the time interval 1550–1750 CE with respect to the 0–1850 CE means. The dark box represents the Sea of Okhotsk region (50–65°N, 135–170°E).

Figure 5. Southern California oxygen minimum zone (OMZ) variability and ventilation sources. (a) Medieval Climate Anomaly (MCA): OMZ intensification coeval with strong connections (in-phase $\delta^{15}N_{sed}$ between SBB and Pescadero) with southern-sourced Equatorial Pacific Intermediate Water (EqPIW) that transports denitrified waters from the Eastern Tropical North Pacific (ETNP); (b) early Little Ice Age (LIA): OMZ relaxation under well ventilated North Pacific Intermediate Water (NPIW) associated with enhanced sea ice formation in the Sea of Okhotsk; (c) late LIA (especially 1600–1750): OMZ intensification associated with weakened EqPIW influences (out-of-phase $\delta^{15}N_{sed}$ responses between SBB and Pescadero) and less ventilated NPIW due to reduced sea ice formation in the Sea of Okhotsk driven by atmospheric forcing.

Acknowledgements and Data

We would like to acknowledge Dorothy Pak and Arndt Schimmelmann, as well as the crew members for R/V Sproul for collecting the cores. This work is supported by the National Science Foundation under grant number OCE-1304327 awarded to I.H.; Y.W. acknowledges support from the Rackham Graduate School of the University of Michigan and the Scott Turner Award. We thank Angela Dial for lab assistance. All geochemical data are archived in the NOAA National Centers for Environmental Information - Paleoclimatology Data (https://www.ncdc.noaa.gov/paleo-search/study/33676).

References

Altabet, M.A. et al., 1999. The nitrogen isotope biogeochemistry of sinking particles from the margin of the Eastern North Pacific. Deep Sea Research I, 46(1999): 655-679.

Anderson, L., Abbott, M.B., Finney, B.P., Burns, S.J., 2005. Regional atmospheric circulation change in the North Pacific during the Holocene inferred from lacustrine carbonate oxygen isotopes, Yukon Territory, Canada. Quaternary Research, 64(01): 21-35.

Bailey, H.L. et al., 2018. Holocene atmospheric circulation in the central North Pacific: A new terrestrial diatom and δ18O dataset from the Aleutian Islands. Quaternary Science Reviews, 194: 27-38.

Barron, J.A., Bukry, D., Hendy, I.L., 2015. High-resolution paleoclimatology of the Santa Barbara Basin during the Medieval Climate Anomaly and early Little Ice Age based on diatom and silicoflagellate assemblages in Kasten core SPR0901-02KC. Quaternary International, 387: 13-22.

Behl, R.J., Kennett, J.P., 1996. Brief interstadial events in the Santa Barbara basin, NE Pacific, during the past 60 kyr. Nature, 379(6562): 243-246.

Berelson, W.M. et al., 2005. Anaerobic diagenesis of silica and carbon in continental margin sediments: Discrete zones of TCO2 production. Geochimica et Cosmochimica Acta, 69(19): 4611-4629.

Bishop, J.K.B., 1988. The barite-opal-organic carbon association in oceanic particulate matter. Nature, 332(6162): 341-343.

Bograd, S.J., 2002. Bottom water renewal in the Santa Barbara Basin. Journal of Geophysical Research, 107(C12).

Bopp, L. et al., 2013. Multiple stressors of ocean ecosystems in the 21st century: projections with CMIP5 models. Biogeosciences, 10(10): 6225-6245.

Bostock, H.C., Opdyke, B.N., Williams, M.J.M., 2010. Characterising the intermediate depth waters of the Pacific Ocean using δ13C and other geochemical tracers. Deep Sea Research Part I: Oceanographic Research Papers, 57(7): 847-859.

Breitburg, D. et al., 2018. Declining oxygen in the global ocean and coastal waters. Science, 359(6371).

Calvert, S.E., Pedersen, T.F., 2007. Elemental Proxies for Palaeoclimatic and Palaeoceanographic Variability in Marine Sediments: Interpretation and Application, Developments in Marine Geology, pp. 567-644.

Cannariato, K.G., Kennett, J.P., 1999. Climatically related millennial-scale fluctuations in strength of California margin oxygen-minimum zone during the past 60 k.y. Geology, 27(11): 975-978.

Carstensen, J., Andersen, J.H., Gustafsson, B.G., Conley, D.J., 2014. Deoxygenation of the Baltic Sea during the last century. Proc Natl Acad Sci U S A, 111(15): 5628-33.

Checkley, D.M., Barth, J.A., 2009. Patterns and processes in the California Current System. Progress in Oceanography, 83(1-4): 49-64.

Crusius, J., Calvert, S., Pedersen, T., Sage, D., 1996. Rhenium and molybdenum enrichments in sediments as indicators of oxic, suboxic and sulfidic conditions of deposition. Earth and Planetary Science Letters, 145: 65-78.

Crusius, J., Pedersen, T.F., Kienast, S., Keigwin, L., Labeyrie, L., 2004. Influence of northwest Pacific productivity on North Pacific Intermediate Water oxygen concentrations during the Bølling-Ållerød interval (14.7–12.9 ka). Geology, 32(7): 633.

Davis, C.V. et al., 2019. Ongoing Increase in Eastern Tropical North Pacific Denitrification as Interpreted Through the Santa Barbara Basin Sedimentary δ15N Record. Paleoceanography and Paleoclimatology, 34(9): 1554-1567.

Deutsch, C. et al., 2014. Centennial changes in North Pacific anoxia linked to tropical trade winds. Science, 345(6197): 665-668.

Du, X., Hendy, I., Schimmelmann, A., 2018. A 9000-year flood history for Southern California: A revised stratigraphy of varved sediments in Santa Barbara Basin. Marine Geology, 397: 29-42.

Dymond, J., Suess, E., Lyle, M., 1992. Barium in Deep-Sea Sediment: A Geochemical Proxy for Paleoproductivity. Paleoceanography, 7(2): 163-181.

Eagle, M., Paytan, A., Arrigo, K.R., van Dijken, G., Murray, R.W., 2003. A comparison between excess barium and barite as indicators of carbon export. Paleoceanography, 18(1).

Erickson, B.E., Helz, G.R., 2000. Molybdenum(VI) speciation in sulfidic waters: stability and lability of thiomolybdates. Geochimica et Cosmochimica Acta, 64(7): 1149-1158.

Evans, Z.C. et al., 2020. The role of water masses in shaping the distribution of redox active compounds in the Eastern Tropical North Pacific oxygen deficient zone and influencing low oxygen concentrations in the eastern Pacific Ocean. Limnology and Oceanography.

Fisler, J., Hendy, I.L., 2008. California Current System response to late Holocene climate cooling in southern California. Geophysical Research Letters, 35(9).

Ganeshram, R.S., François, R., Commeau, J., Brown-Leger, S.L., 2003. An experimental investigation of barite formation in seawater. Geochimica et Cosmochimica Acta, 67(14): 2599-2605.

Gingele, F.X., Zabel, M., Kasten, S., Bonn, W.J., Nürnberg, C.C., 1999. Biogenic Barium as a Proxy for Paleoproductivity: Methods and Limitations of Application. In: Fischer, G., Wefer, G. (Eds.), Use of Proxies in Paleoceanography: Examples

from the South Atlantic. Springer Berlin Heidelberg, Berlin, Heidelberg, pp. 345-364.
Goericke, R., Bograd, S.J., Grundle, D.S., 2015. Denitrification and flushing of the Santa Barbara Basin bottom waters. Deep Sea Research Part II: Topical Studies in Oceanography, 112: 53-60.
Griffith, E.M., Paytan, A., 2012. Barite in the ocean - occurrence, geochemistry and palaeoceanographic applications. Sedimentology, 59(6): 1817-1835.
Hakim, G.J. et al., 2016. The last millennium climate reanalysis project: Framework and first results. Journal of Geophysical Research: Atmospheres, 121(12): 6745-6764.
Hamill, T.M., Whitaker, J.S., Snyder, C., 2001. Distance-Dependent Filtering of Background Error Covariance Estimates in an Ensemble Kalman Filter. Monthly Weather Review, 129(11): 2776-2790.
Harrison, B.K., Zhang, H., Berelson, W., Orphan, V.J., 2009. Variations in archaeal and bacterial diversity associated with the sulfate-methane transition zone in continental margin sediments (Santa Barbara Basin, California). Appl Environ Microbiol, 75(6): 1487-99.
Hendy, I.L., 2010. Diagenetic behavior of barite in a coastal upwelling setting. Paleoceanography, 25(4).
Hendy, I.L., Dunn, L., Schimmelmann, A., Pak, D.K., 2013. Resolving varve and radiocarbon chronology differences during the last 2000 years in the Santa Barbara Basin sedimentary record, California. Quaternary International, 310: 155-168.
Hendy, I.L., Napier, T.J., Schimmelmann, A., 2015. From extreme rainfall to drought: 250 years of annually resolved sediment deposition in Santa Barbara Basin, California. Quaternary International, 387: 3-12.
Hendy, I.L., Pedersen, T.F., 2005. Is pore water oxygen content decoupled from productivity on the California Margin? Trace element results from Ocean Drilling Program Hole 1017E, San Lucia slope, California. Paleoceanography, 20(4): 1-12.
Itaki, T., 2004. Middle to late Holocene changes of the Okhotsk Sea Intermediate Water and their relation to atmospheric circulation. Geophysical Research Letters, 31(24).
Ivanochko, T.S., Pedersen, T.F., 2004. Determining the influences of Late Quaternary ventilation and productivity variations on Santa Barbara Basin sedimentary oxygenation: a multi-proxy approach. Quaternary Science Reviews, 23(3-4): 467-480.
Keigwin, L.D., 1998. Glacial-age hydrography of the far northwest Pacific Ocean. Paleoceanography, 13(4): 323-339.
Kienast, S.S., Calvert, S.E., Pedersen, T.F., 2002. Nitrogen isotope and productivity variations along the northeast Pacific margin over the last 120 kyr: Surface and subsurface paleoceanography. Paleoceanography, 17(4): 7-1-7-17.
Kimura, N., 2004. Increase and decrease of sea ice area in the Sea of Okhotsk: Ice production in coastal polynyas and dynamic thickening in convergence zones. Journal of Geophysical Research, 109(C9).
Koizumi, I., Shiga, K., Irino, T., Ikehara, M., 2003. Diatom record of the late Holocene in the Okhotsk Sea. Marine Micropaleontology, 49(1): 139-156.

Kuwabara, J.S., Geen, A.V., Mccorkle, D.C., Bernhard, J.M., 1999. Dissolved sulfide distributions in the water column and sediment pore waters of the Santa Barbara Basin. Geochimica et Cosmochimica Acta, 63(15): 2199-2209.

Liu, K.-K., Kaplan, I.R., 1989. The eastern tropical Pacific as a source of 15N ‐ enriched nitrate in seawater off southern California. Limnology and Oceanography, 34(5): 820-830.

Martin, S., Drucker, R., Yamashita, K., 1998. The production of ice and dense shelf water in the Okhotsk Sea polynyas. Journal of Geophysical Research: Oceans, 103(C12): 27771-27782.

McManus, J. et al., 1998. Geochemistry of barium in marine sediments: implications for its use as a paleoproxy. Geochimica et Cosmochimica Acta, 62(21): 3453-3473.

McManus, J., Berelson, W.M., Klinkhammer, G.P., Kilgore, T.E., Hammond, D.E., 1994. Remobilization of barium in continental margin sediments. Geochimica et Cosmochimica Acta, 58(22): 4899-4907.

Miyao, T., Ishikawa, K., 2003. Formation, distribution and volume transport of the North Pacific Intermediate Water studied by repeat hydrographic observations. Journal of Oceanography, 59(6): 905-919.

Moffitt, S.E., Hill, T.M., Ohkushi, K., Kennett, J.P., Behl, R.J., 2014. Vertical oxygen minimum zone oscillations since 20 ka in Santa Barbara Basin: A benthic foraminiferal community perspective. Paleoceanography, 29(1): 44-57.

Moffitt, S.E., Hill, T.M., Roopnarine, P.D., Kennett, J.P., 2015. Response of seafloor ecosystems to abrupt global climate change. Proc Natl Acad Sci U S A, 112(15): 4684-9.

Napier, T.J., Hendy, I.L., Fahnestock, M.F., Bryce, J.G., 2019. Provenance of detrital sediments in Santa Barbara Basin, California, USA: Changes in source contributions between the Last Glacial Maximum and Holocene. GSA Bulletin.

Neukom, R. et al., 2019. Consistent multidecadal variability in global temperature reconstructions and simulations over the Common Era. Nature Geoscience, 12(8): 643-649.

Neukom, R., Steiger, N., Gómez-Navarro, J.J. et al. No evidence for globally coherent warm and cold periods over the preindustrial Common Era. Nature 571, 550–554 (2019).

Ohkushi, K. et al., 2013. Quantified intermediate water oxygenation history of the NE Pacific: A new benthic foraminiferal record from Santa Barbara basin. Paleoceanography, 28(3): 453-467.

Okazaki, Y. et al., 2006. Cycladophora davisiana (Radiolaria) in the Okhotsk Sea: a key for reconstructing glacial ocean conditions. Journal of Oceanography, 62: 639-648.

Osterberg, E.C. et al., 2014. Mount Logan ice core record of tropical and solar influences on Aleutian Low variability: 500–1998 A.D. Journal of Geophysical Research: Atmospheres, 119(19): 11189-11204.

Osterberg, E.C. et al., 2017. The 1200 year composite ice core record of Aleutian Low intensification. Geophysical Research Letters, 44(14): 7447-7454.

PAGES 2k Consortium, 2017. A global multiproxy database for temperature reconstructions of the Common Era. Sci Data, 4: 170088.

PAGES 2k Consortium, 2013. Continental-scale temperature variability during the past two millennia. Nature Geoscience, 6(5): 339-346.

Parkinson, C.L., 1990. The Impact of the Siberian High and Aleutian Low on the Sea-Ice Cover of the Sea of Okhotsk. Annals of Glaciology, 14: 226-229.

Paytan, A., Griffith, E.M., 2007. Marine barite: Recorder of variations in ocean export productivity. Deep Sea Research Part II: Topical Studies in Oceanography, 54(5-7): 687-705.

Raven, M.R., Sessions, A.L., Fischer, W.W., Adkins, J.F., 2016. Sedimentary pyrite δ34S differs from porewater sulfide in Santa Barbara Basin: Proposed role of organic sulfur. Geochimica et Cosmochimica Acta, 186: 120-134.

Reid, J.L., 1965. Intermediate waters of the Pacific Ocean. Johns Hopkins Oceanography Studies, 5: 1-96.

Reimer, P.J. et al., 2013. IntCal13 and Marine13 radiocarbon age calibration curves 0–50,000 years cal BP. Radiocarbon, 55(4): 1869-1887.

Reimers, C.E., Ruttenberg, K.C., Canfield, D.E., Christiansen, M.B., Martin, J.B., 1996. Porewater pH and authigenic phases formed in the uppermost sediments of the Santa Barbara Basin. Geochimica et Cosmochimica Acta, 60(21): 4037-4057.

Riedinger, N., Kasten, S., Gröger, J., Franke, C., Pfeifer, K., 2006. Active and buried authigenic barite fronts in sediments from the Eastern Cape Basin. Earth and Planetary Science Letters, 241(3-4): 876-887.

Rodionov, S.N., Bond, N.A., Overland, J.E., 2007. The Aleutian Low, storm tracks, and winter climate variability in the Bering Sea. Deep Sea Research Part II: Topical Studies in Oceanography, 54(23-26): 2560-2577.

Schimmelmann, A. et al., 1992. Extreme climatic conditions recorded in Santa Barbara Basin laminated sediments: the 1835–1840 Macoma event. Marine Geology, 106(1992): 279-299.

Scott, C. et al., 2008. Tracing the stepwise oxygenation of the Proterozoic ocean. Nature, 452(7186): 456-9.

Shcherbina, A.Y., Talley, L.D., Rudnick, D.L., 2004a. Dense water formation on the northwestern shelf of the Okhotsk Sea: 1. Direct observations of brine rejection. Journal of Geophysical Research: Oceans, 109(C9).

Shcherbina, A.Y., Talley, L.D., Rudnick, D.L., 2004b. Dense water formation on the northwestern shelf of the Okhotsk Sea: 2. Quantifying the transports. Journal of Geophysical Research: Oceans, 109(C9).

Shimada, C., Ikehara, K., Tanimura, Y., Hasegawa, S., 2004. Millennial-scale variability of Holocene hydrography in the southwestern Okhotsk Sea: diatom evidence. The Holocene, 14(5): 641-650.

Skrivanek, A., Hendy, I.L., 2015. A 500 year climate catch: Pelagic fish scales and paleoproductivity in the Santa Barbara Basin from the Medieval Climate Anomaly to the Little Ice Age (AD 1000–1500). Quaternary International, 387: 36-45.

Steiger, N.J., Hakim, G.J., Steig, E.J., Battisti, D.S., Roe, G.H., 2014. Assimilation of Time-Averaged Pseudoproxies for Climate Reconstruction. Journal of Climate, 27(1): 426-441.

Stramma, L., Schmidtko, S., Levin, L.A., Johnson, G.C., 2010. Ocean oxygen minima expansions and their biological impacts. Deep Sea Research Part I: Oceanographic Research Papers, 57(4): 587-595.

Tachibana, Y., Honda, M., Takeuchi, K., 1996. The Abrupt Decrease of the Sea Ice over the Southern Part of the Sea of Okhotsk in 1989 and Its Relation to the Recent Weakening of the Aleutian Low. Journal of the Meteorological Society of Japan. Ser. II, 74(4): 579-584.

Talley, L.D., 1993. Distribution and formation of North Pacific Intermediate Water. Journal of Geophysical Oceanography, 23: 517-537.

Tardif, R. et al., 2019. Last Millennium Reanalysis with an expanded proxy database and seasonal proxy modeling. Climate of the Past, 15(4): 1251-1273.

Tems, C.E., Berelson, W.M., Prokopenko, M.G., 2015. Particulate δ15N in laminated marine sediments as a proxy for mixing between the California Undercurrent and the California Current: A proof of concept. Geophysical Research Letters, 42(2): 419-427.

Tems, C.E. et al., 2016. Decadal to centennial fluctuations in the intensity of the eastern tropical North Pacific oxygen minimum zone during the last 1200 years. Paleoceanography, 31(8): 1138-1151.

Tessin, A., Chappaz, A., Hendy, I., Sheldon, N., 2018. Molybdenum speciation as a paleo-redox proxy: A case study from Late Cretaceous Western Interior Seaway black shales. Geology, 47(1): 59-62.

Torres, M.E., Brumsack, H.J., Bohrmann, G., Emeis, K.C., 1996. Barite fronts in continental margin sediments: a new look at barium remobilization in the zone of sulfate reduction and formation of heavy barites in diagenetic fronts. Chemical Geology, 127(1): 125-139.

Tribovillard, N., Algeo, T.J., Lyons, T., Riboulleau, A., 2006. Trace metals as paleoredox and paleoproductivity proxies: An update. Chemical Geology, 232(1-2): 12-32.

Von Breymann, M.T., Emeis, K.-C., Suess, E., 1992. Water depth and diagenetic constraints on the use of barium as a palaeoproductivity indicator. Geological Society, London, Special Publications, 64(1): 273.

Wagner, M., Chappaz, A., Lyons, T.W., 2017. Molybdenum speciation and burial pathway in weakly sulfidic environments: Insights from XAFS. Geochimica et Cosmochimica Acta, 206: 18-29.

Wang, Y., Hendy, I., Napier, T.J., 2017. Climate and Anthropogenic Controls of Coastal Deoxygenation on Interannual to Centennial Timescales. Geophysical Research Letters, 44(22): 11528–11536.

Wang, Y., Hendy, I.L., Thunell, R., 2019. Local and Remote Forcing of Denitrification in the Northeast Pacific for the Last 2,000 Years. Paleoceanography and Paleoclimatology.

Wang, Y., Hendy, I.L., Zhu, J., 2020. Expansion of the Southern California oxygen minimum zone during the early-to mid-Holocene due to reduced ventilation of the Northeast Pacific. Quaternary Science Reviews, 238.

Warrick, J.A., Farnsworth, K.L., 2009. Sources of sediment to the coastal waters of the Southern California Bight. The Geological Society of America Special Paper, 454: 39-52.

Watanabe, T., Wakatsuchi, M., 1998. Formation of 26.8–26.9 σθ water in the Kuril Basin of the Sea of Okhotsk as a possible origin of North Pacific Intermediate Water. Journal of Geophysical Research: Oceans, 103(C2): 2849-2865

Yasuda, I., 1997. The origin of the North Pacific Intermediate Water. Journal of Geophysical Research, 102(C1): 893.

You, Y., 2003. The pathway and circulation of North Pacific Intermediate Water. Geophysical Research Letters, 30(24).

You, Y. et al., 2000. Roles of the Okhotsk Sea and Gulf of Alaska in forming the North Pacific Intermediate Water. Journal of Geophysical Research, 105(C2): 3253.

You, Y. et al., 2003. Transport of North Pacific Intermediate Water across Japanese WOCE sections. Journal of Geophysical Research, 108(C6).

Zheng, Y., Anderson, R.F., Geen, A.V., James, K., 2000. Authigenic molybdenum formation in marine sediments: A link to pore water sulfide in the Santa Barbara Basin. Geochimica et Cosmochimica Acta, 64(24): 4165-4178.

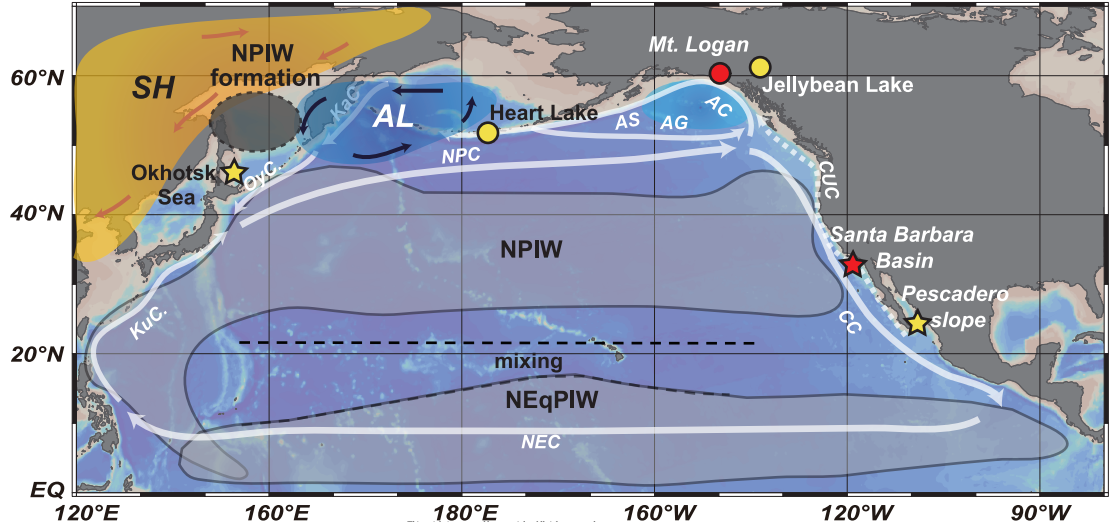

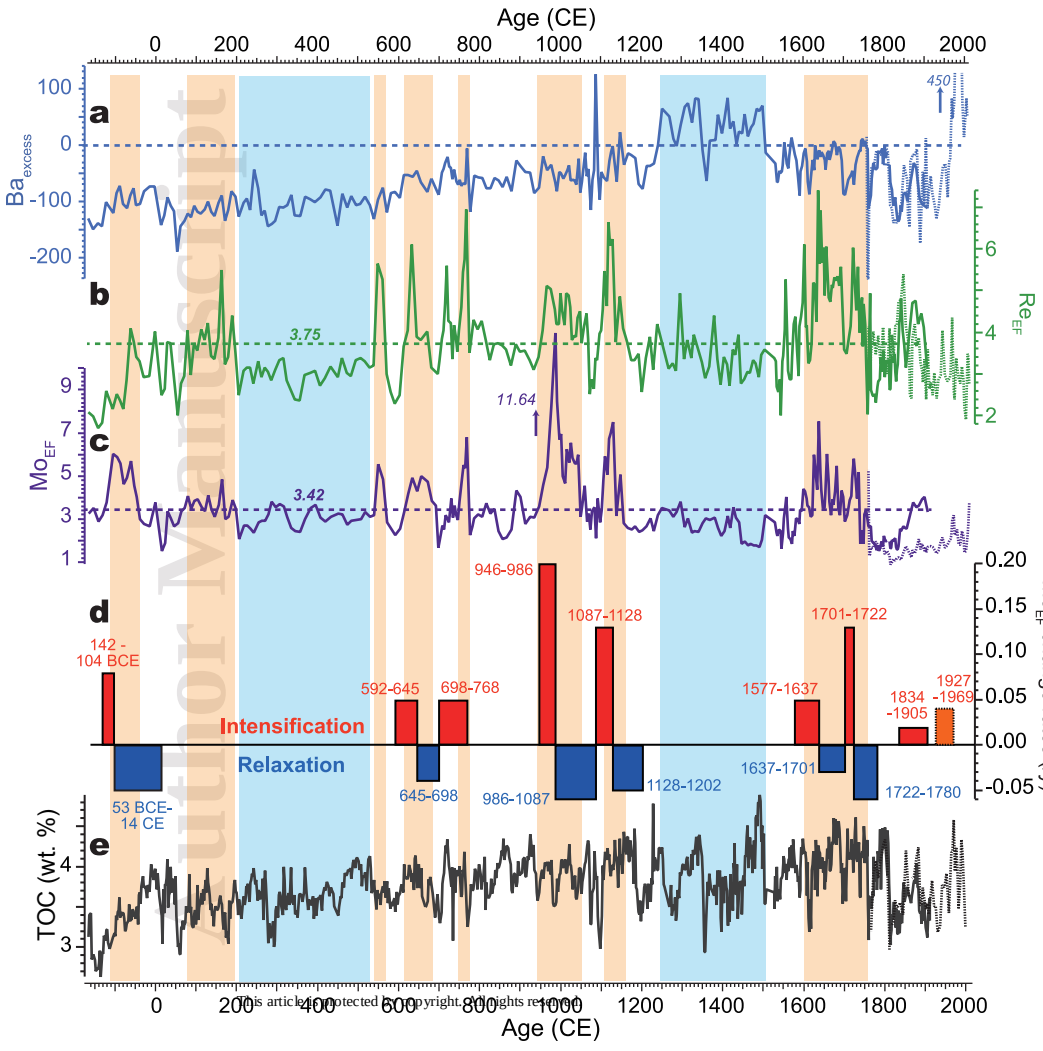

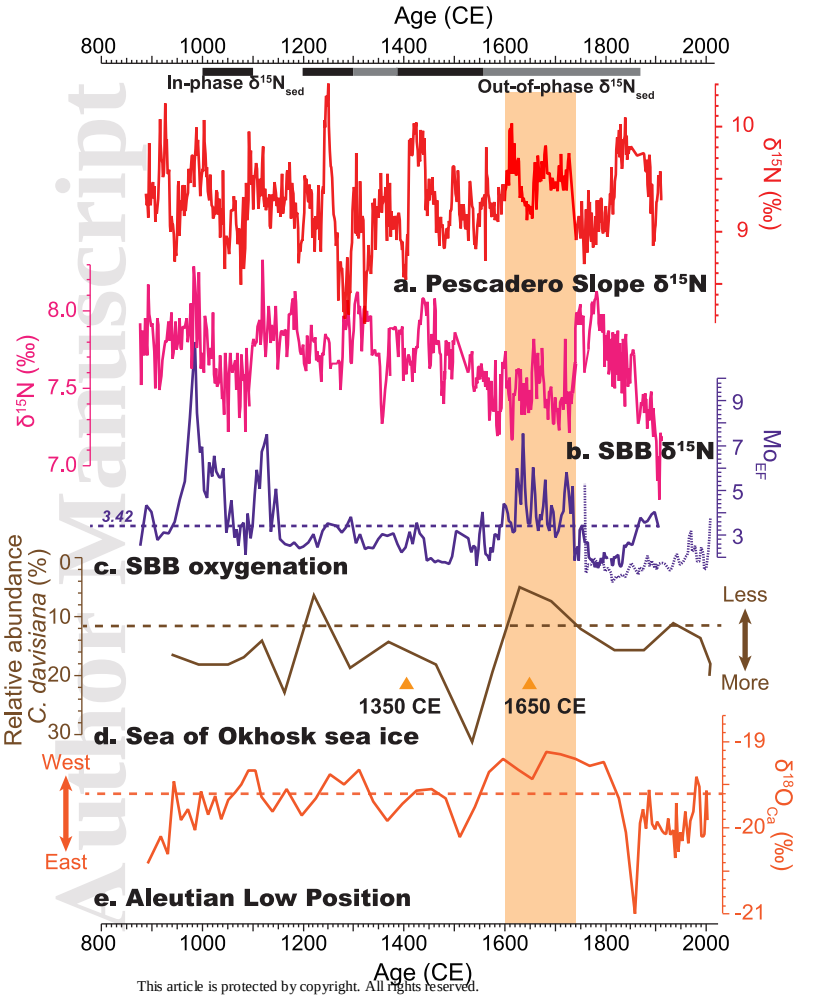

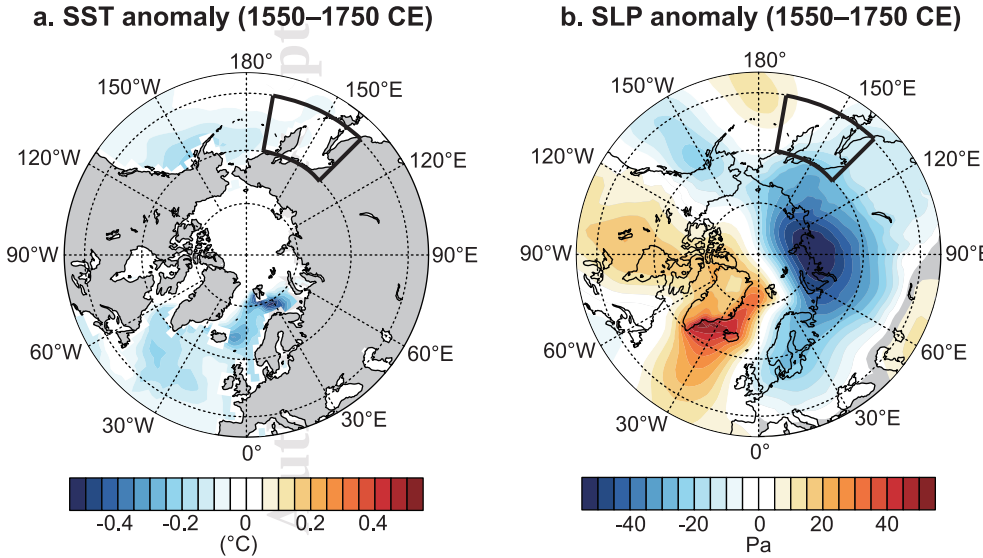

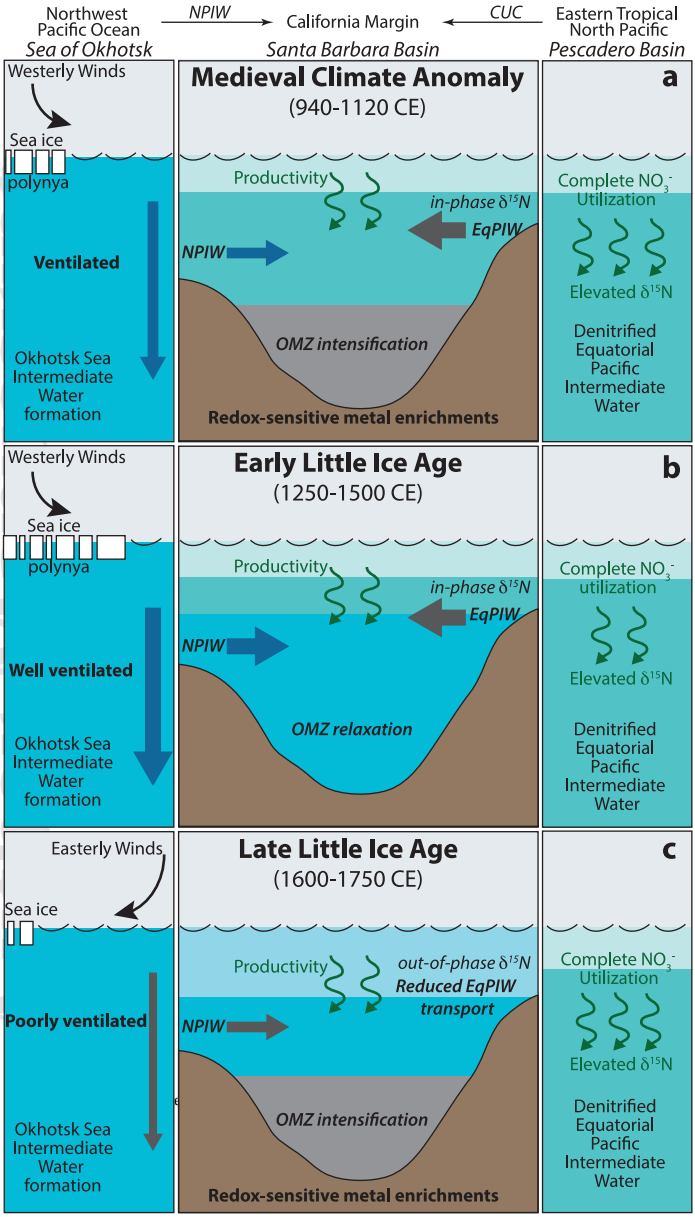
Northwest Pacific Ocean
Sea of Okhotsk
NPIW
California Margin
Santa Barbara Basin
CUC
Eastern Tropical North Pacific
Pescadero Basin
Westerly Winds
Sea ice
polynya
Ventilated
Okhotsk Sea Intermediate Water formation
Medieval Climate Anomaly
(940-1120 CE)
Productivity
in-phase δ15N
EqPIW
NPIW
OMZ intensification
Redox-sensitive metal enrichments
a
Complete NO3- Utilization
Elevated δ15N
Denitrified Equatorial Pacific Intermediate Water
Westerly Winds
Sea ice
polynya
Well ventilated
Okhotsk Sea Intermediate Water formation
Early Little Ice Age
(1250-1500 CE)
Productivity
in-phase δ15N
EqPIW
NPIW
OMZ relaxation
b
Complete NO3- utilization
Elevated δ15N
Denitrified Equatorial Pacific Intermediate Water
Easterly Winds
Sea ice
Poorly ventilated
Okhotsk Sea Intermediate Water formation
Late Little Ice Age
(1600-1750 CE)
Productivity
out-of-phase δ15N
Reduced EqPIW transport
NPIW
OMZ intensification
Redox-sensitive metal enrichments
c
Complete NO3- Utilization
Elevated δ15N
Denitrified Equatorial Pacific Intermediate Water